PLASMONIC NANOSTRUCTURES FOR SURFACE-ENHANCED RAMAN SPECTROSCOPY

by

RUIQIAN JIANG

Presented to the Faculty of the Graduate School of

The University of Texas at Arlington in Partial Fulfillment

of the Requirements

for the Degree of

MASTER OF SCIENCE IN MATERIALS SCIENCE AND ENGINEERING

THE UNIVERSITY OF TEXAS AT ARLINGTON

August 2014

Acknowledgements

I would like to thanks for those people who have helped me to accomplish my thesis during my master's study. First of all, I would like to acknowledge my advisor Dr.Yaowu Hao, for his instruction, guidance and inspiration for both my research and adaption to life in Arlington, Texas. I was very lucky there were so many excellent members, Kevin, Koi, Alex, Sina and James, in our group, and they provided their kind help without any reservation when I needed it most. This research and thesis would not have been completed on schedule without their patient assistance.

Moreover, my thanks to CCMB and Nanofab, where they provide most of advanced facilities for my project. I also appreciate Dr.Fuqiang Liu and Dr. Digant P.Dave for serving in my thesis committee.

Last but not least, I want to show my gratitude to my parents and my wife. Sincere thanks to my parents for their financial support and to my wife who took good care of my daily needs, supporting me during my long hours in the lab and studying.

July. 15th, 2014

Abstract

PLASMONIC STRUCTURES FOR SURFACE ENHANCED RAMAN SCATTERING SPECTROSCOPY

Ruiqian Jiang, M.S.

The University of Texas at Arlington, 2014

Supervising Professor: Yaowu Hao

In the last three decades, a large number of different plasmonic nanostructures have attracted much attention due to their unique optical properties. Those plasmonic nanostructures include nanoparticles, nanoholes and metal nanovoids. They have been widely utilized in optical devices and sensors.

When the plasmonic nanostructures interact with the electromagnetic wave and their surface plasmon frequency match with the light frequency, the electrons in plasmonic nanostructures will resonate with the same oscillation as incident light. In this case, the plasmonic nanostructures can absorb light and enhance the light scattering.

Therefore, the plasmonic nanostructures can be used as substrate for surface-enhanced Raman spectroscopy to enhance the Raman signal. Using plasmonic nanostructures can significantly enhance Raman scattering of molecules with very low concentrations.

In this thesis, two different plasmonic nanostructures Ag dendrites and Au/Ag core-shell nanoparticles are investigated. Simple methods were used to produce these two plasmonic nanostructures. Then, their applications in surface enhanced Raman scattering have been explored.

Ag dendrites were produced by galvanic replacement reaction, which was conducted using Ag nitrate aqueous solution and copper metal. Metal copper layer was deposited at the bottom side of anodic aluminum oxide (AAO) membrane. Silver wires formed inside AAO channels connected Ag nitrate on the top of AAO membrane and copper layer at the bottom side of AAO. Silver dendrites were formed on the top side of AAO.

The second plasmonic nanostructure is Au/Ag core-shell nanoparticles. They were fabricated by electroless plating (galvanic replacement) reaction in a silver plating solution. First, electrochemically evolved hydrogen bubbles were used as template through electroless deposition to produce hollow Au nanoparticles. Then, the Au nanoparticles were coated with Cu shells in a Cu plating solution. In the following step, a

AgCN based plating solution was used to replace Cu shell to form Au/Ag core-shell nanoparticles.

These two plasmonic nanostructures were tested as substrates for Raman spectroscopy. It demonstrated that these plasmonic nanostructures could enhance Raman signal from the molecules on their surface. The results indicate that these plasmonic nanostructures could be utilized in many fields, such as such as biological and environmental sensors.

Table of Contents

List of Illustrations

List of Tables

Chapter 1

Introduction

In the last decade, plasmonic nanostructures are rapidly becoming attractive research topics in different areas due to their unique optical properties [1]. The growing research field studying the interaction between electromagnetic wave and metal surface interaction is called “Plasmonics”[2]. Plasmonic materials are usually metals or metal-like materials that have negative real permittivity dispersion. Most plasmonic nanostructures are gold and silver nanostructures, which show unique optical property in visible light wavelength ranges[3]. A large number of different plasmonic nanostructures have been fabricated and investigated in the last two decades. They include nanoparticles, nanoholes, nanotubes, crystal dendrites and metal nanovoid arrays. Moreover, different strategies modifying the surfaces of these materials make it possible to affect the selective binding and detection of specific targets for chemical and biological sensing.[4] This plasmonic research field attracted much attention due to its potential applications in optical devices, sensors, diagnostics and therapeutics in the biology field[5, 6].

Surface plasmons are a coherent oscillation of conduction electrons on a metal surface excited by electromagnetic radiation on the metal nanostructures. This phenomenon occurs in the nanoscale dimension. When metal nanostructures interact with light, which can be considered as an

oscillating electric field, the free conduction electrons inside nanostructures will oscillate driven by the electric field. These free conduction electrons have their own oscillation frequency, which is called surface plasmon resonance frequency (SPR). SPR is dependent on the size and shape of the nanostructures. When the light irradiate on such metal nanostructures (the light is an electromagnetic wave with its own oscillating frequency). The electrons will resonate with the light when SPR frequency and light frequency match. Therefore, the incident light at SPR frequency will strongly be absorbed and scattered. In other words, the electric field of incident light will be enhanced. This novel phenomenon provides a promising technique for sensing and identifying molecular species.

Raman spectroscopy is a powerful technique to identify the molecular species since most molecules have their own distinct spectrum. With different unique vibrational frequencies. Raman scattering is aninelastic scattering of a photon interacting with a molecule. The energy of photons will change when interacting with the molecules. However, a Raman scattering signal is very weak for very low concentration molecules; only one in 10^{12} photons could undergo Raman scattering[7]. In other words, Raman signals are weak to detect in general; there are a low number of photons available to detect. So, Raman spectroscopy is a great tool only for the high concentration molecules.

Thirty years ago, Martin Fleischmann found that the pyridine molecules could have significantly enhanced Raman signal when adsorbed on electrochemically roughened Ag metal surface. [8] This initial publication has been cited 3698 times. This phenomenon can be explained and referred to as Surface Enhanced Raman Spectroscopy (SERS) as showed in the Figure 1-1. It is a surface-sensitive technique; only molecules adsorbed on the roughened metal surface would have enhanced Raman scattering. Since then, surface-enhanced Raman spectroscopy has become one of the primary tools in analytical and surface research with enormous promises for high sensitive detection for very low concentration molecules. The enhancement factors would reach 10^{10} to 10^{11}.

SERS utilizes nanoscale metal surfaces typically made of gold (Au) or silver (Ag). Laser excitation of these metal nanostructures would drive the surface charges creating a highly localized (plasmonic) light field. When a molecule is absorbed close to the enhanced field at the surface, a large enhancement of the Raman signal can be observed. Raman signals several orders of magnitude greater than normal Raman scattering are common. The Raman signal can be amplified further when laser light is matched to the absorption maxima of the molecules. This effect is known as Surface-Enhanced Resonance Raman scattering effect (SERRS).

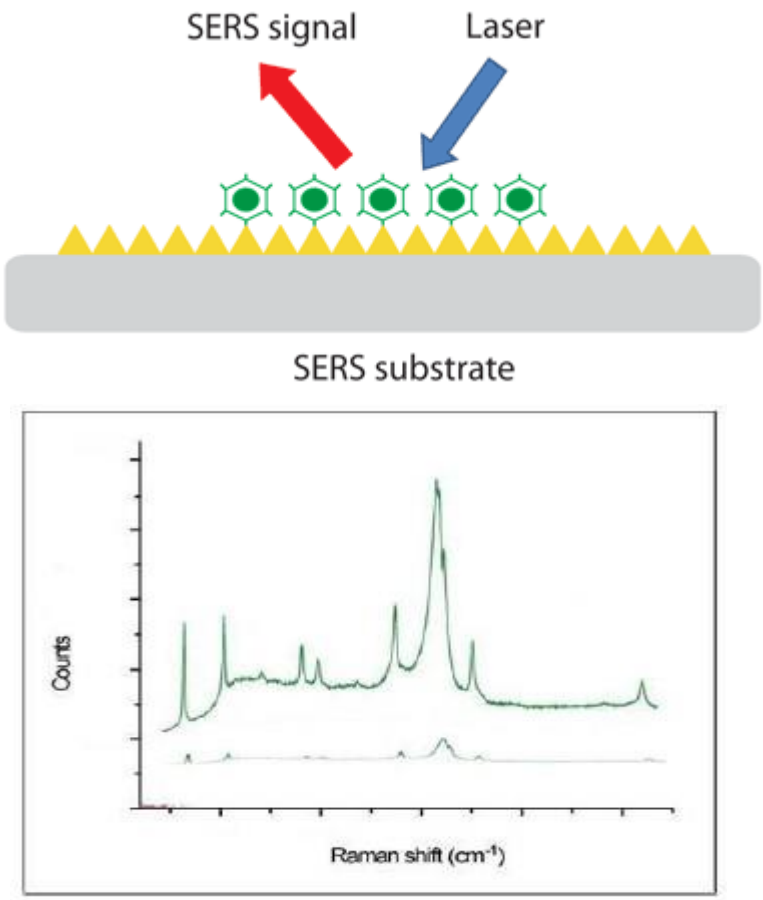

Figure 1- 1 Illustration of Surface-Enhanced Raman Spectroscopy

SERS is a great technique that has been used in a variety of fields and applications, such as detection of the presence of low concentration of biomolecules, detection of proteins in body fluids [9], analysis for chemistry testing, detection of trace amounts of chemical and biological agents, drug detection, food quality analysis and single cell detection[10].

In this thesis, two different palsmonic nanostructures Ag dendrites and Au/Ag core-shell nanoparticles were fabricated by two simple methods. These unique plasmonic nanostructures can amplify Raman signals for low concentration molecules. Their plasmonic properties and formation mechanisms of nanostructures were investigated in this project.

Chapter 2

Background Information

In this chapter, fundamental knowledge of plasmonics, including surface plasmon resonance, plasmonic nanostructures and their applications are first introduced. Then, the principle of Raman scattering and Surface-enhanced Raman spectroscopy are presented.

2.1 Plasmonic Nanostructures

In the last decade, research in plasmonic nanostructures is becoming an attractive field due to its potential applications in many areas[9]. The plasmonic properties depend on metallic nanostructure's size and shape because there are some interacting processes between electromagnetic radiation and conduction electrons on the surface of nanostructures[11]. With efforts from scientists in different areas, plasmonic nanostructures are now used in the optical device, photonic circuits and sensors as well as in medical diagnostics[12]. Especially, plasmonic nanostructures found some applications in Raman spectroscopy used in the nanoscale biosensing for DNA recognize [13], detecting protein-protein interactions[14] and chemical sensing [15] due to their advantages of label-free, low cost and real-time monitoring[16].

2.1.1 Fundamental Plasmon Properties

Plasmon is a collective oscillation of the free electrons in metal nanostructures. For example, when one metal particle is in a uniform electron field, electrons inside particle moves from one side to the other side. Then the electrons will move back to the original position driven by the attractive force. To visualize a plasmon oscillation, we can assume that a cube of metal was put in the external electric field. The conduction electrons will move from one side to the other side. With both external electric field and charged electrons being changed, which causes the “overshoot” phenomenon[17]. As a result, the electrons will oscillate back and forth at a specific frequency, which is called plasma frequency. And Plasmon is a quantization of these oscillation movements.

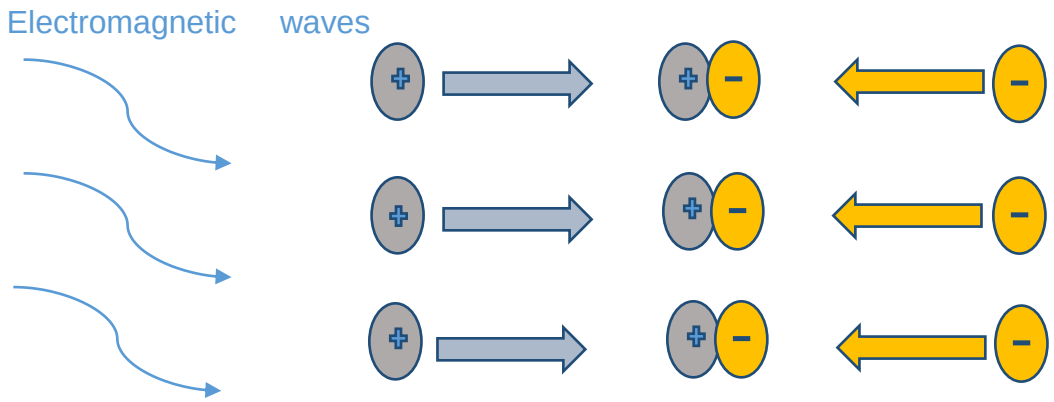

Figure 2- 1 Scheme of Plasma Oscillation in a Metal Particle Induced by Electromagnetic Wave

Plasmon materials have been playing an appealing role in the optical properties of metal nanostructures. Usually metals are highly reflective materials due to their plasma frequency which lies in the ultraviolet spectrum which is higher than the frequency of visible light. Metals such as copper and gold, have electronic inter band transitions in the visible range, so they have their particular colors.

The position and intensity of plasmon absorption are highly affected by the surface property of the materials. For the surface features including modification of plasmonic structures' shape, morphology and size, they could build different plasmonic modes. These plasmonic modes have brought a good understanding of surface plasmon resonance, which is an important

phenomenon in the optical field. The following chapter will present background information and principles of surface plasmon resonance.[18]

2.1.2 Principle of Surface Plasmon Resonance (SPR)

Generally, surface plasmon resonance (SPR) refers to the electrons that will stimulate oscillation in a metal when the incident electromagnetic waves shine it. Specifically, it is a nanoscale size effect of the interaction between the electromagnetic waves and electrons[19]. We can assume that there is a box of free electrons placed inside an oscillating electric field. These free electrons will oscillate from one side to the other side driven by the electric field. With these regular movements, the free electrons have their own frequency. The electromagnetic wave of light irradiating to this box has its frequency. When the frequencies between free electrons and electromagnetic wave of light match, the oscillation of free electrons will move farther and their amplitude dramatically increase. As a result, the absorption of light by such metal particles will be increased. This is so-called plasmon resonance effect.

For metal nanoparticles, if the size of nanoparticles is much smaller than the wavelength of the light, the collective oscillation of plasma would be localized near the surface. Also the resonance frequency would shift from the plasma frequency to the surface plasmon resonance frequency[20]. For

metals including Au, Ag and Cu. SPR peaks of their nanoparticles are in the visible region. At SPR frequency, these nanoparticles strongly enhance the scattering and absorption of the visible and near infrared(NIR) lights.[21]. Taking gold nanoparticles as an example, the SPR peaks of gold nanoparticles with diameter about 50 to 100nm are are centered at around 550nm.

To better understand this surface plasmon phenomenon, here the first Maxwell equation and Gauss's law are introduced, which can be expressed as:

$$\nabla \times D = \rho_f$$

where D is the electric displacement; ρ_f is the free charge density.

We can suppose that the size of the particle is much smaller than the wavelength of light and the particles are homogeneous. Under the electric fields, the Laplace equation can be used to obtain the potentials inside and outside the particles.

$$\phi_{in} = -\frac{3\varepsilon_m}{\varepsilon + 2\varepsilon_m} E_0 r \cos\theta \qquad (2\text{-}1)$$

$$\phi_{out} = -E_0 r \cos\theta + \frac{p}{4\pi\varepsilon_0 \varepsilon_m r^2} \qquad (2\text{-}2)$$

where ε_m is the dielectric constant of medium and ε is dielectric constant of the metal sphere; E_0 is external field and r is position vector at point P; *a* is radius of the sphere; *p* is the dipole moment with the form:

$$p = 4\pi\varepsilon_0\varepsilon_m a^3 \frac{\varepsilon - \varepsilon_m}{\varepsilon + 2\varepsilon_m} E_0 \qquad (2\text{-}3)$$

Also we can refer polarizability *α* through $p = \alpha\varepsilon_0\varepsilon_m E_0$, then α can written as:

$$\alpha = 4\pi a^3 \frac{\varepsilon - \varepsilon_m}{\varepsilon + 2\varepsilon_m} \qquad (2\text{-}4)$$

Therefore, the equation above could be re-written as:

$$\alpha = (1+\kappa)\varepsilon\Omega \frac{\varepsilon - \varepsilon_m}{\varepsilon + (1+\kappa)\varepsilon_m} \qquad (2\text{-}5)$$

where Ω is referred to the volume of the particle. I It is obvious that dipolar polarizability *α* could get the biggest value when $\mathrm{Re}[\varepsilon(\omega)] = -\kappa\varepsilon_m$, while κ is referred to a shape factor, which represents geometrical polarizability for the surface. We can use the electron oscillations to explain it. Tiny nanostructures shape factor would have an enhancement of dipolar polarizability, which can explain why they could enhance LSPR intensity[22].

According to these rules of plasmons, the exact size of nanoparticles should be considered when trying to get a significant enhancement of absorption and scattering in the experiments. Therefore, synthesis of new

nanostructures is an important process to the further research in the plasmonics field.

In summary, SPR in nanometer-sized structures is called Localized Surface Plasmon Resonance (LSPR). LSPR is collective free electron charge oscillations in metal nanoparticles that are stimulated by electromagnetic waves. When the surface resonance happens, the metal nanoparticles displayed strongly enhanced near-field amplitude. Even though far-field scattering by the nanoparticles is also enhanced by the resonance, this field is localized to the nanoparticles and disappears quickly from the nanoparticles interface into the dielectric background.

2.2 Raman Spectroscopy and Surface Enhanced Raman Scattering

2.2.1 Raman Spectroscopy

Raman spectroscopy is a spectroscopic tool used to examine vibrational and low frequency modes in a system. Raman spectroscopy is used as an analysis tool for chemical sensing through the vibrational excitation from the interaction of laser beam with molecules. The interaction between laser beam and molecules result in the energy of the laser photons being shifted up or down. The shift in energy gives information about the vibrational modes in the system.

When molecules are irradiated by electromagnetic radiation of a single frequency, the light will be scattered by the molecules both elastically and inelastically. Elastic scattering is known as Rayleigh scattering and inelastic scattering is called Raman scattering.

Raman scattering is typically very weak. The light can be treated as an electromagnetic wave and molecule treated as tiny sphere connected by the spring as shown in the Figure 2-2.

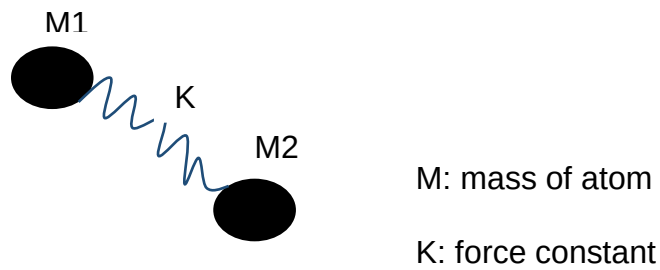

Figure 2- 2 Model Molecule in Raman System

The energy of incident light is

$$E(x,t) = E_0 \cos(wt - kx)$$

When a molecule is placed in the electric field, it generates an induced dipole moment because its positively charged nuclei are attached toward the

negative pole and its electrons are attracted toward the positive pole of the field[23]. Polarizability is a measurement of capability of inducing a dipole moment in an electric field. Which is based on the molecule structure and structure bonds.

The strength of dipole moment is

$$P = \alpha E$$

E can be given by

$$E = E_0 \cos(2\pi V_0 t)$$

where V_0 is incident light frequency. Substituting these above equations to give induced dipole moment

$$P = \alpha E_0 \cos(2\pi V_0 t)$$

For most molecular bonds, the single atoms are restricted to specific vibrational modes. The vibrational energy of mode is expressed as

$$E_{vib} = \left(j + \frac{1}{2}\right) h V_{vib}$$

Where j is vibrational quantum number, V_{vib} is the frequency of the vibrational mode, and h is Planck constant[24].

While the matters were illuminated by the incident light, the electromagnetic wave will stimulate dipole moment oscillation. Usually, the vibrational quanta is smaller than the energy level of the virtual state. There

are two possible outcomes of scattering during the interaction of photons and molecules, the material will absorb or lose energy and emit the photons. When the photons have a lower energy than the absorbed photon energy, this phenomenon is called Stokes Raman scattering. On the contrary, when the photons have a higher energy than the absorbed photons energy, the consequence is called as anti-Stokes Raman scattering. The Raman scattering contains both Stokes scattering and anti- Stokes scattering. As shown in the Figure 2-3. It is scattering from an individual molecule or atom and results from electric polarizability of the atoms.

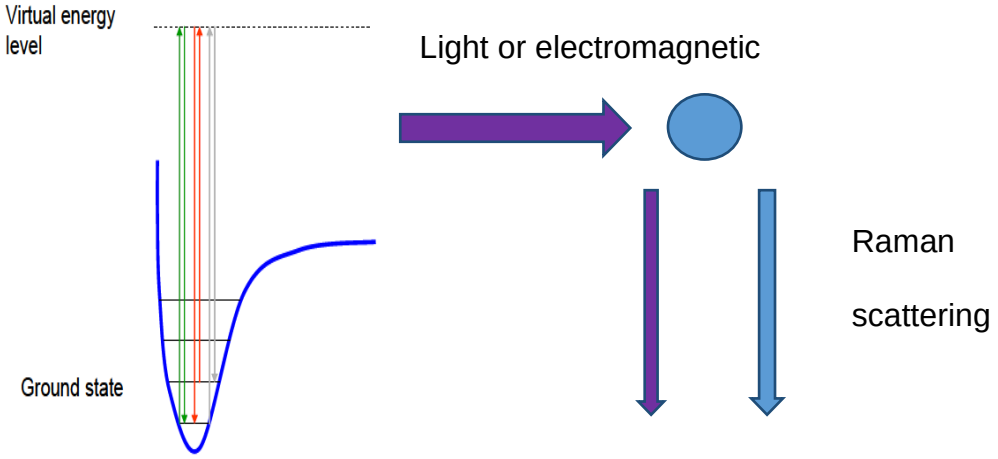

Figure 2- 3 Energy Level Diagram for the Ground State and the Virtual Energy Level and Scattering from Interaction of Light and Molecules

To be Raman active, a vibration mode needs to result in polarizability change in a molecule. Polarizability determines the deformability of the electron cloud of a molecule in an external electric field. So polarizability is a critical factor for the Raman scattering.

Raman microscopes are a commonly used tool for material characterization. Raman microscopes can examine microscopic area of material by illuminated laser beam down to the micrometer level. This tool should be referred to as Raman microspectroscope because Raman microscope is not primarily used for imaging purposes.

Raman spectroscopy needs to collect a spectrum from each wavenumbers separately, it is different from FTIR that collects a spectrum in a range of wavenumbers. Raman microscopy is the same as those of conventional dispersive Raman instruments, which include the following elements:

1. Laser source
2. Illumination and collection system
3. Spectral analyzer
4. Detection and computer control system[25]

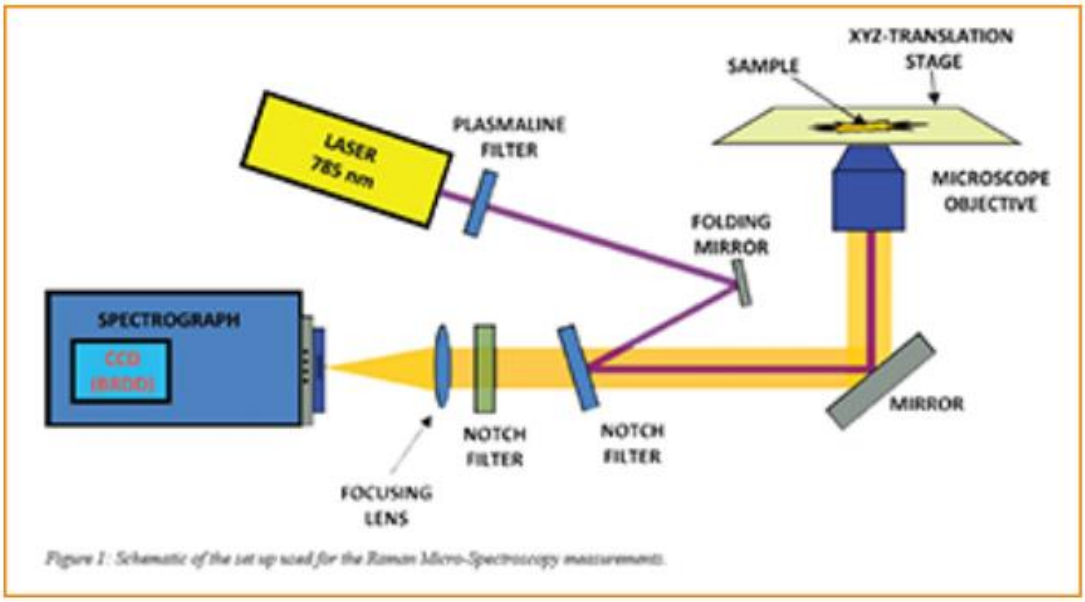

Figure 2- 4 Schematic of Raman Spectroscope

Raman spectroscopy needs to use highly monochromatic light illuminating to the sample, which can be provided by the laser source.Laser source usually used are gas continuous wave lasers such as Ar, Kr and He-Ne. These laser sources are able to generate beams with different wavelengths. Also, the laser source can easily generate several tens of mW of laser power.

The optical arrangement of Raman microscopic system is illustrated in the Figure 2-4.

A filter can be used to make laser beam become a single wavelength beam, which is then illuminated on a sample surface by microscope. The microscope can collect the Raman scattered light reflected from the sample

surface. This scattered light will travel to the detector. The Raman scattered light results from inelastic scattering, which is weak compared with the incident laser light. Thus, the filter can be used here for the purpose of blocking the laser light entering the detection system. In order to eliminate elastically scattered light, the light from the microscope has to pass through a special filter before the light reaches the analyzer. The Raman scattering is difficult to detect without the filters, because the intensity of elastically of scattering is higher than inelastically scattered Raman light.

The important component of the spectral analyzer in the system is diffracting grating. Before these signals are recorded by the detector, the diffracting grating is used to select the wavelength of Raman scattering. It is used to disperse Raman scattered light depending on the wavenumbers of light. There are some fine parallel grooves on the surface of the diffraction grating that are used to equally dispersed wavenumbers of light. When the light shines the diffraction grating, the grating disperses the light with discrete direction. The function of diffraction grating in the system is similar to that of equal-spaced atomic planes in crystals for X-ray diffraction.

The detector is used to record different wavelengths of Raman scattered light. It is made from photoelectric materials. The detector is able to convert photon signals to electric signals. The most commonly used detector is a charge-coupled device (CCD) detector. A CCD detector is made from

silicon-based semiconductor photosensitive elements. It can record and detect intensity of different wavelengths distributed by the diffraction grating. The computer is used to calculate and plot the Raman shift with versus wavenumber for the Raman spectrum.

The biggest limitation of Raman spectroscopy is a fluorescence problem due to the fact colored samples and impurities might absorb laser radiation and emit it again as fluorescence. The intensity of fluorescence can be as much as 10000 times higher than Raman scattered light. Hence, the intensity of fluorescence signal might cover the Raman scattered signal completely. Three methods can be used to minimize fluorescence:

1. Illuminating the material using high-power laser beam with prolonged time can make the impurity fluorescence bleached out.
2. Using a longer wavelength to change the wavelength of laser excitation.
3. An electron gate can be used to measure the Raman signal. Because Raman scattering lifetime is much shorter than fluorescence[26].

2.2.2 Surface-enhanced Raman Spectroscopy

Surface-enhanced Raman scattering (SERS) was observed in University of Southampton, UK, in 1973 by Martin Fleischman et.al[27]. It was found that when the molecules adsorbed the electrochemically roughed silver rod, they can get a more than million times enhanced Raman signal. Afterwards, some people proposed that excitation of surface plasmon can be used to explain this huge enhancement. Currently, surface-enhanced Raman spectroscopy is a powerful tool used to detect the signal from the interaction of molecules with light. Importantly, this useful tool furthers the development of some novel devices based on the plasmonic nanostructures.

Both electromagnetic and electronic fields are important for the SERS effect[28]. According to electromagnetic theory, the direction of electric field intensity in the metal surface will change because the resonant effect between the surface plasmon and optical fields. Hence, the Raman signal can be greatly enhanced when the SPR frequency of particles match the light frequency. The type, shape, size and distribution of metal particles and the frequency of incident light are major factors that affect the Raman enhancement. When the frequency of incident electromagnetic wave and frequency of scattering light are the same as the plasmon frequency it can result in a huge enhancement. In addition, SERS can occur in a variety of morphologies of metal particles.

Typically, the metal nanoparticles can be used for the SERS measurement. There are a lot of metal particles with different size and shape that can be used, especially from the silver, gold and copper metal particles. Molecules generally are adsorbed onto the first layer of metal surface, and the enhancement effect has tens of nanometers range for the Raman measurements[27].

The fabrication of SERS substrate and SERS active materials has become a challenge facing to researchers in this area. SERS active materials include a large number of transition metals and metal semiconductors[29]. Different SERS substrates can offer some key information to explain the SERS mechanism.

The physical principal of SERS is based on the conventional description of Raman effect[30]. Typically, the enhancement signal is produced from the changes of the electric field. The SERS enhancement is extremely strong when both the incident and scattering fields are resonated with the plasmon frequency. It has been found that when the shape of metal structure was sharp it would enhance Raman signal strongly. Also, the electric field would greatly enhance Raman signal for the Raman system when two or more particles accumulate together[31].

However, some experiments indicate that some enhancements are not from the electric field, they might be from another reason. A good

example to illustrate this phenomenon is the study of SERS from CO and N_2 by Moskovit [17]. The chemistry plays an important role in this situation, it indicates that the cross section of two gas phases are almost similar, while the SERS signal from these two gas phase are very different under the same condition. The enhancement from CO is about two or three orders of magnitude greater than the enhancements of N_2[32].

2.3 Plasmonic Nanostructures for SERS Substrate

Recently, surface enhanced Raman spectroscopy (SERS) has become a useful analytical tool for improvement of chemical analysis and biology sensors [33]. However, there is a challenge for producing uniform, reproducible and highly sensitive SERS substrates [10, 19, 30, 34]. On the other hand, Plasmonic nanostructures have been attracting a lot of attention in the nanoscience and nanotechnology field. In the past two decades, there were plenty of different types of plasmonic nanostructures that have been synthesized, characterized and utilized in different areas. [22, 34, 35].

Investigating the synthesis of nanostructures has been a hot topic of research due to their important applications in different areas including photothermal, optoelectronics, biological sensing and medical therapies. Now, people can control their size and morphology to control their electronic and catalytic properties of metal nanoparticles. There are so many literatures

focused on the synthesis of plasmonic nanostructures with well-controlled size and shapes. Generally, there are two methods, top-down and bottom-up, were used to produce nanostructures.

Raman enhancement occurs when the molecules attach to the surface of metal nanoparticles. There are ‘hot spots’ existing the surface owing to the surface plasmon resonance and the electromagnetic field varying on the surface of metal nanoparticles[36]. Design of maximum hot spots of metal nanoparticles is an important principal for SERS design. Recently, there are a lot of designs of 1D and 2D SERS substrates that have been reported through controlling the shape and size of metal or bimetallic nanostructures [37].

The size and shape of plasmonic nanostructures are two big factors strongly influencing the enhancement. After so many efforts in the SERS research field, the ideal size for metal nanoparticles and ideal thickness of surface for SERS has been found. Usually, the bigger size will lead to a lower overall efficiency of the enhancement. However, if metal nanoparticles are too small, they will fail to produce electrical conductivity and fail to have an enhancement in the electric field. Also, high large area and high uniformity are important factors when preparing SERS substrates.

Chapter 3

Ag Dendrites Nanostructures

In this chapter, the fabrication process, and mechanism of formation of Ag dendrites on the top of AAO are discussed. Then, its plasmonic properties and SERS results are presented.

3.1 Synthesis of Ag Dendrites on the Top of AAO Membrane

3.1.1. Deposition of Cu Thin Film on the Bottom Side of AAO.

We utilized Anodic Aluminum Oxide (AAO) membrane to separate the reactant metal Cu layer and product Ag, producing completely free standing Ag dendrites. Commercial AAO filter (from Whatman International Corp.) were used as a substrate. The thickness of AAO is about 60 um and the diameter of channels various from 20 nm to 200 nm. The bottom side of AAO side was sputter-deposited with a 500nm Cu thin film by a thermal evaporator (Figure 3-1 as shown for NRC 3117) in the Nanofab cleanroom.

The chamber of the thermal evaporator was first pumped down to 10^{-3} Torr through a mechanical pump. And then, the cryo pump could generate a vacuum lower than 10^{-5} Torr . The deposition rate is 3 angstrom per second.

Figure 3- 1 Thermal Evaporator NRC 3117 Used for Deposition Cu Thin Film on One Side of AAO

3.1.2 Galvanic Replacement Method To Produce Silver Dendrites

First, the silicon wafer was washed by an Ethanol solution and dried under a soft stream of nitrogen gas, which was used to provide a flat stage to place AAO membrane during the experiments. In order to make AAO membrane affix on the silicon wafer completely, we dropped a little bit of deionize water into the interface between the silicon wafer and Cu-deposited side of AAO.

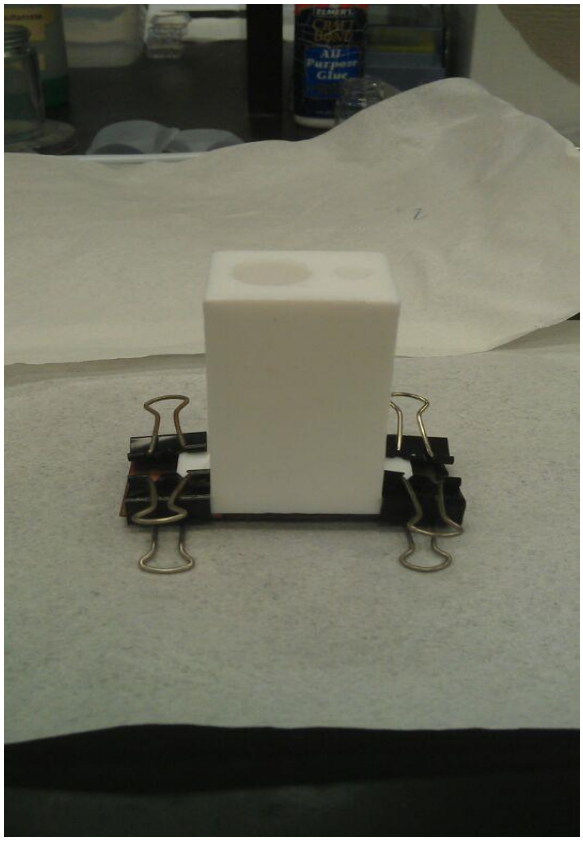

Figure 3- 2 Home-Made Three Electrode Cell

Then, as shown in the Figure 3-2, a sealed cell was placed on the top of the AAO membrane. $AgNO_3$ solution was poured into the cell. In this way, $AgNO_3$ solution can only reach to the Cu surface through channels of the AAO membrane. In this case, $AgNO_3$ solution and Cu thin film were separated by AAO membrane. To our surprise, we could obtain very pure and highly ordered Ag dendrites on the top AAO surface without connecting to the bottom Cu film. After fomation of Ag dendrites, membranes were

immersed into Deionize water for thirty minutes, and then be washed and dried in air.

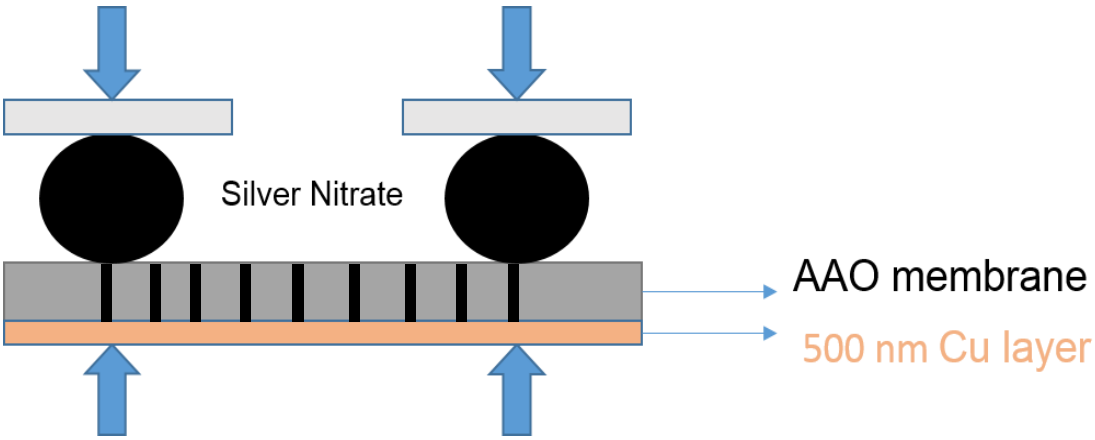

Figure 3- 3 Schematic of Set up Fabrication Silver Dendrites

3.1.3 Mechanism of Forming Ag Dendrites on The Top of AAO Membran

Here, the mechanism of forming Ag dendrites on the top of AAO mambrane was discussed. From the Figure 3-4, we can definitely see there are Ag wires inside of AAO membrane channel. Ag wires inside the AAO membrane channel conect the Cu on the bottom side to the Ag on the top side. The electrons can move from the Cu layer on the bottom to the Ag. The bottom side reaction is:

$$Cu \rightarrow Cu^{2+} + 2e^{-}$$

And the top side reaction is :

$$Ag^{+} + e^{-} \rightarrow Ag$$

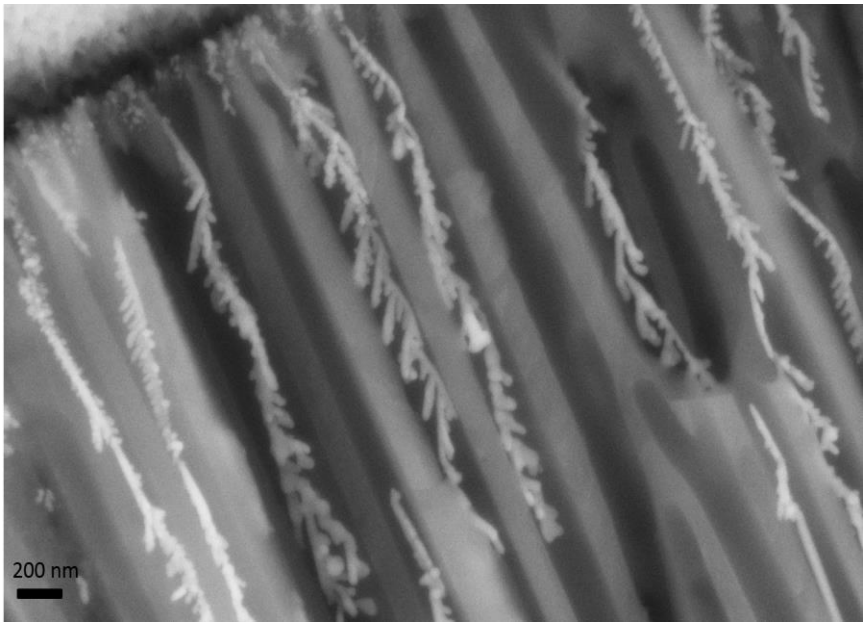

Figure 3- 4 SEM Image of Cross-Section AAO Membrane

We can consider this process as tiny galvanic cell as shown in the Figure 3-5. The ions and electrons can go through the AAO channel and Ag wires. The overall reaction is

$$Cu + AgNO_3 \rightarrow Ag + Cu(NO_3)2$$

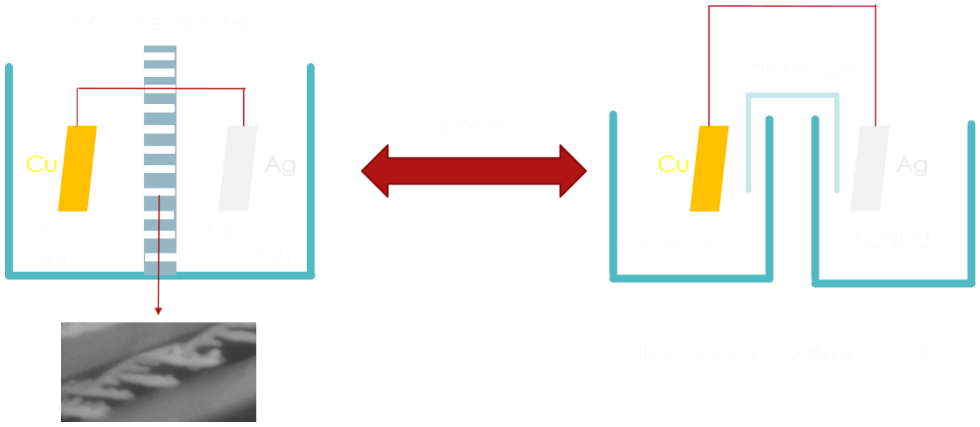

Figure 3- 5 The Experiment Process Is Equivalent with Galvanic Cell

The process for forming Ag dendrites on the top of AAO was further illustrated in the Figure 3-6. The electrons from the Cu layer can go through Ag wires to the top of Ag, they even can reach to the dendrites tip. The Ag ions could obtain electrons to grow Ag from the tip position. As Ag crystal growth prefer to (111) direction, so they can form Ag dendrites on the top of AAO membrane.

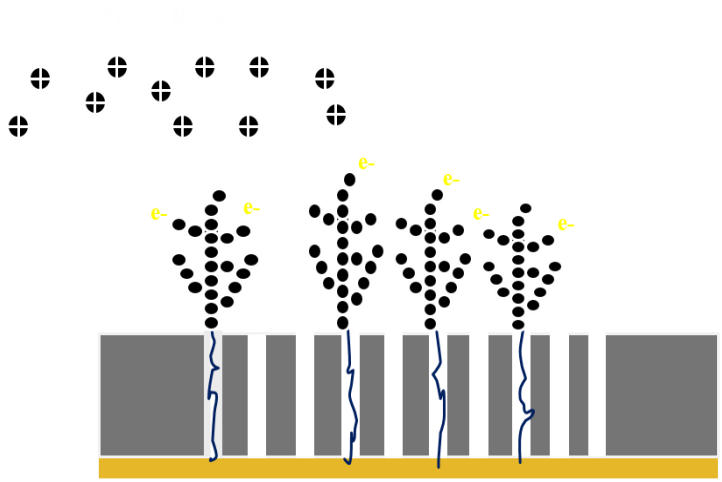

Figure 3- 6 The Process for Forming Ag Dendrites on The Top of AAO Membrane

There are several advantages for this procedure when compared with other methods to produce Ag dendrites. We can obtain a large area, clean Ag dendrites. Most importantly, Ag dendrites can be separated from Cu layer while in all other methods Ag dendrites were connected the Cu metal surface.

3.2 Characterization of Silver Dendrites

3.2.1 Scanning Electron Microscopy

Figure 3-7 shows SEM images of Ag dendrites fabricated at different concentrations with different reaction times. It is primarily dependents on the $AgNO_3$ solution concentration. After instilling 20 mM $AgNO_3$ solutions into AAO top surface for 5 mins, tree-like of Ag drendrites with size around 2 um were aggregated on the top of AAO membrane Figure 3-7 (a). When the concentration of $AgNO_3$ increase to 40mM, the symmetrical dendrites can be obtained as shown in Figure 3-7 (b). However, the Ag dendrites nanostructure were not uniformly distributed on the AAO top membrane with this low concentration. And these nanostructures were insufficient for further measurements. After instilling 100 m mol/L $AgNO_3$ for 5 mins, a layer of Ag dendrites with symmetrical branches were formed. (See Figure 3-7 (c)). This AAO substrate can be used to as SERS substate. From the Figure 3-7 (d), we know that the overall length of the Ag dendrite is 15 um, and both the branches and the stems are 30-50 nm in diameter. It is obvious that the silver dendrites are highly symmetric, and the angles between the stem and branches are mostly 55°. From these SEM images, we can conclude that when the concentration of $AgNO_3$ increases, the Ag dendrite will grow bigger. We can obtain a large amount of Ag dendrites with high concentration of $AgNO_3$ and longer reaction process time.

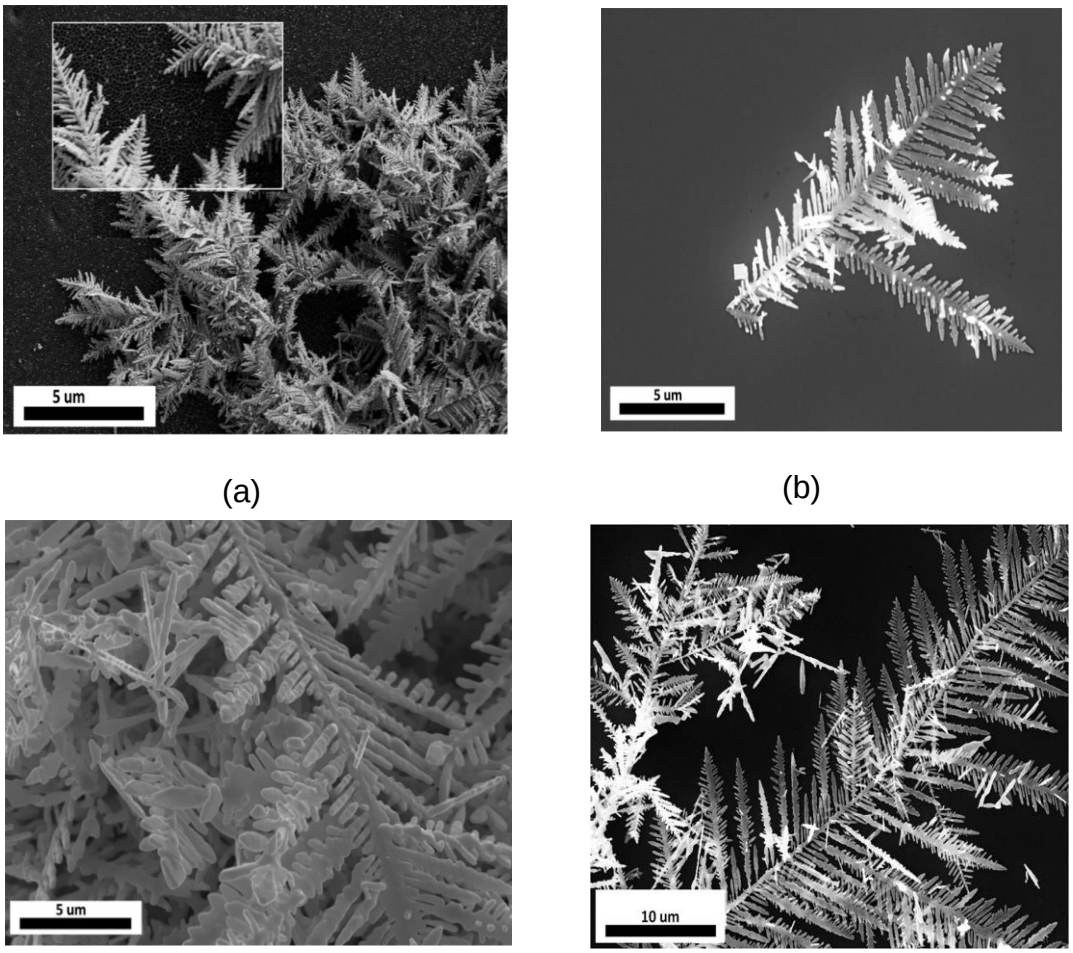

(a) (b)

(c) (d)

Figure 3- 7 SEM Images of Silver Dendrites Made by Galvanic Replacement

3.2.2 X-Ray Diffraction Pattern

Figure 3-8 is an X-ray diffraction pattern of Ag dendrite prepared at 100 mM AgNO3 for 5 mins, indicating that the Ag dendrites are of high crystallinity. There are five diffraction peaks that can be indexed, which are

(111), (200), (220), (311), (222) diffraction peaks of the face-centered cubic (FCC) Ag (JCPDS 65-2871). The sharp diffraction peaks indicate that the symmetric Ag dendrites were highly crystallized. The intensity of (111) peak is very sharp and its intensity is much stronger than other peaks, indicating that silver crystal growth direction are preferentially parallel to the (111) direction. Moreover, it can be seen that this Ag dendrite is one single crystal since their diffraction peaks are very sharp as shown in the figure. This conclusion has been be confirmed in the HRTEM analysis (see later part).

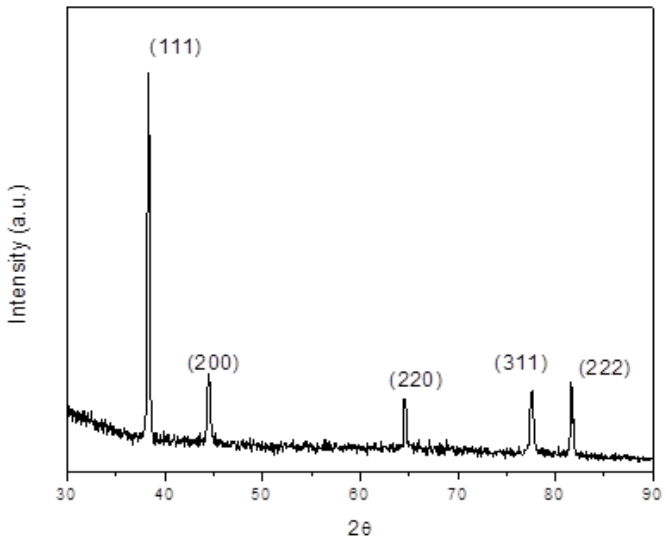

Figure 3- 8 X-Ray Diffraction (XRD) Pattern of Ag Dendrites

Obtained from 100 M M $AgNO_3$ for 5 Mins

3.2.3 Transmission Electron Microscopy Analysis

The nanostructure of Ag dendrites were investigated by HR-TEM. A TEM micrograph of a typical dendritc nanostrcuture is shown in Figure 3-10. The dendrite looks like beautiful leaves and remarkable hierarchical sprawling to several generations with similarity. The whole length of Ag dendrites is 10 um and the diameter of dendrite is about 30 nm. From the selected area electron diffraction pattern and dark field image, it shows that silver dendrite is one single crystal. When stems and branches grow longer and longer, new branches were formed successively in the tip of branches.

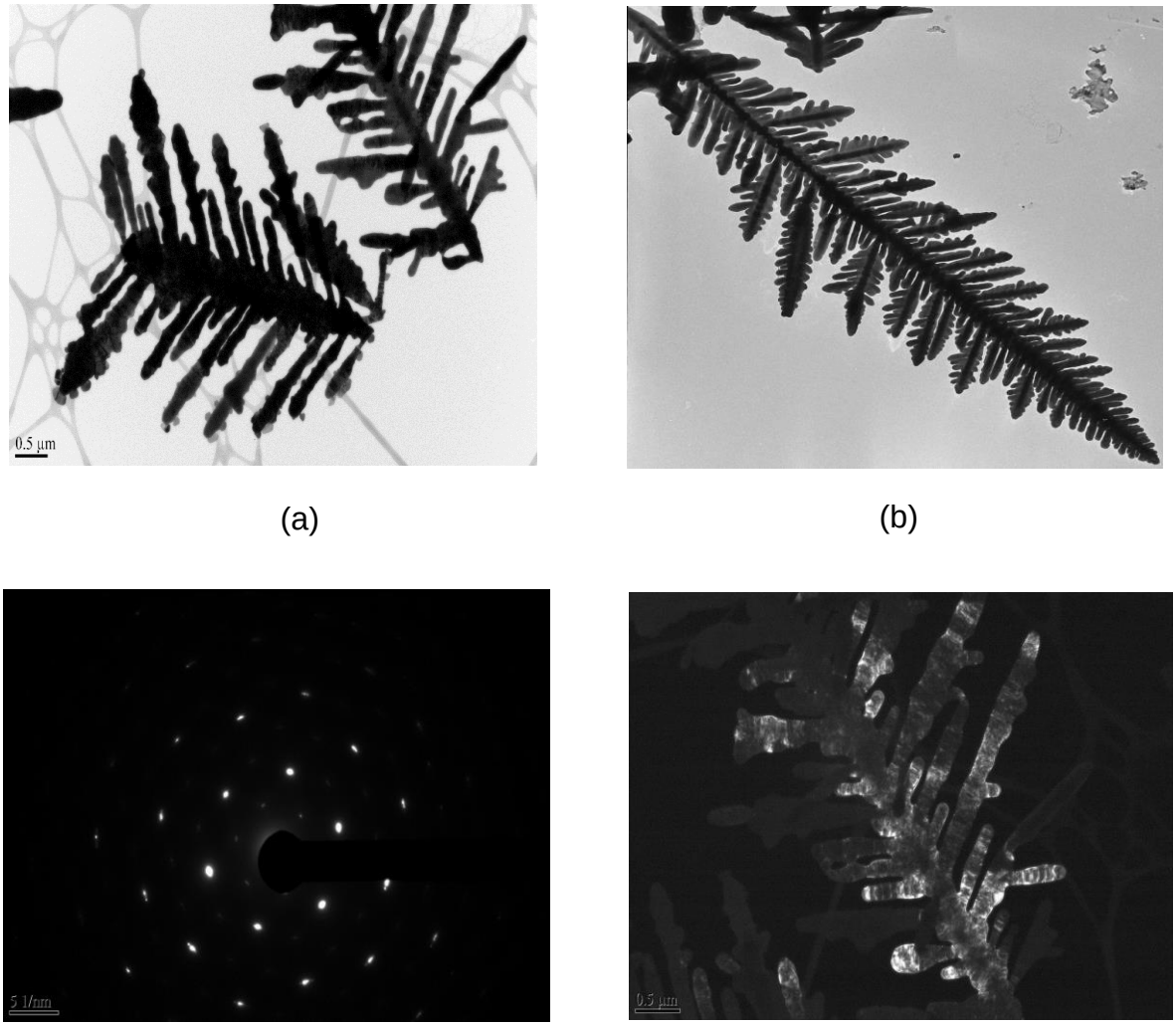

(a) (b)

(c) (d)

Figure 3- 9 (a) and (b) TEM Images of Ag Dendrites Prepared by 100 Mm $AgNO_3$ Solution Reacting with Cu for 30 Seconds. (C) and (D) Electron Diffraction Pattern and Dark Field Image Showing that Ag Dendrite Is Single Crystal.

3.2.5 Plasmonic Properties of Ag Dendrites and SERS Results

After we get a large area of Ag dendrites on the top surface of AAO membrane, the R6G solution with concentration of 1.0×10^{4} M was dropped into Ag dendrites for three hours at the room temperature. Then, the substrates were rinsed with deionized water several times. The preparation process of SERS sample is illustrated in Figure 3-11.

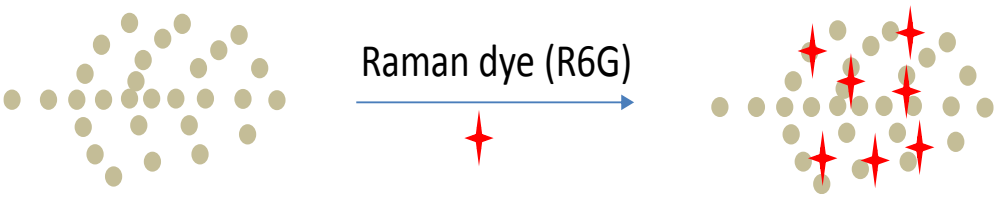

Figure 3- 10 Illustration of the Preparation Process of Raman Sample for Ag Dendrites.

The Raman spectroscopy measurement was conducted using DXR thermo Raman microscopy with a 532 nm laser in CCMB. The signal was collected with 8 s of exposure time and laser power is 50 mW. The Raman spectrum of Ag dendrites with concentration 1×10^{-4} M R6G displayed the

major vibrational modes of R6G at 610, 773, 933, 1041, 1127, 1183, 1275, 1310, 1360, 1420, 1507, 1573, 1573, 1595 and 1648 cm^{-1} as shown in Figure 3-8. From the Raman spectra, it can be seen that a big enhancement was obtained while compared with Raman spectrum of the original R6G dye molecules.

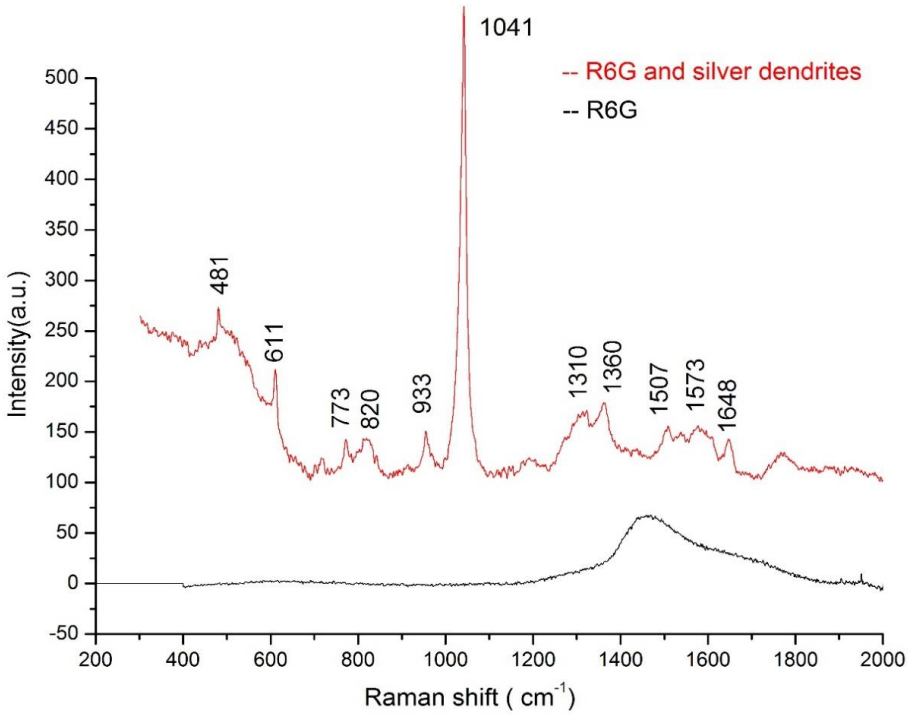

Figure 3- 11 SERS Spectrum of R6G Absorbed on Ag Dendrites on AAO Substrate.

Chapter 4

Au/Ag Core-Shell Nanoparticles

4.1 Synthesis of Au/Ag Core-Shell Nanoparticles

4.1.1 Synthesis of Au Hollow Nanoparticles

For the purpose of making Au/Ag core-shell nanoparticles, the Au hollow nanoparticles were first synthesized. The synthesis method was conducted in a typical three-electrode cell as shown in Figure 4-1.

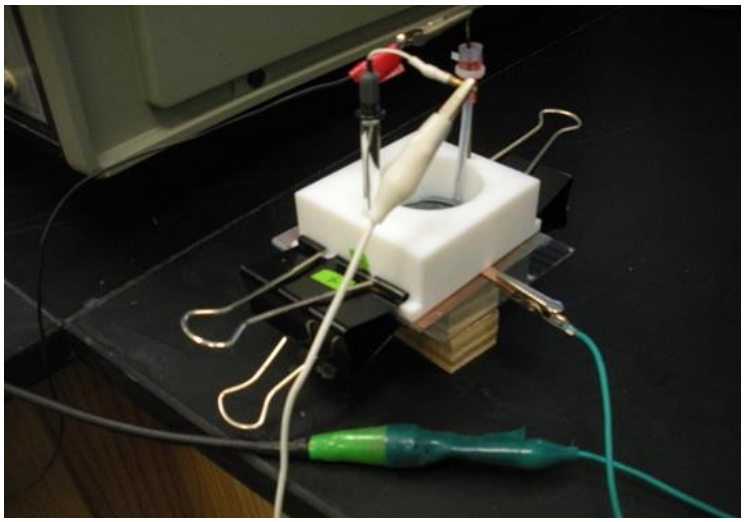

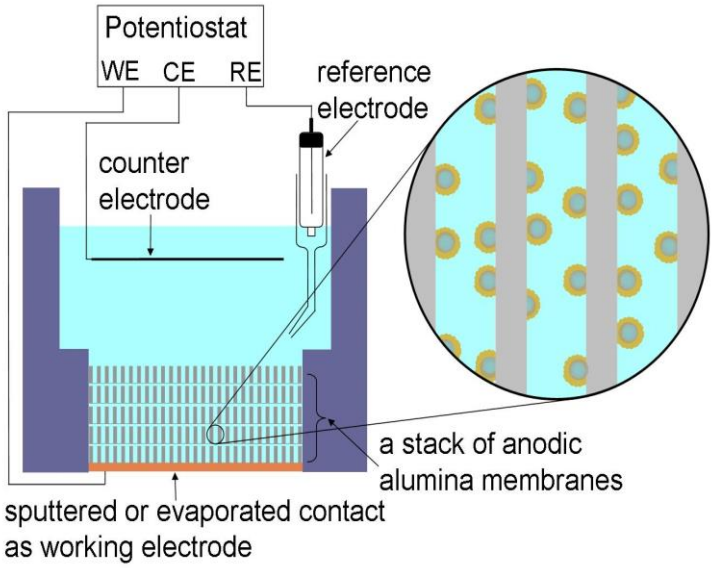

Figure 4- 1 Illustration of Synthesis of Au Hollow

Nanoparticles In the Three-Electrode Electro-deposition Cell

Commercial anodic aluminum oxide (AAO) membranes were used in this synthesis procedure. The electrolyte is a commercial sodium gold sulfite ($Na_3Au(SO3)_2$, PH-7.5) based solution. The electrolyte PH value was adjusted to 6.0 by $NiSO_4$ solution. In this synthesis process, 100 ml commercial Au solution and 25 ml $NiSO_4$ solution were mixed to pour into the 15ml three-electrode cell. Then, electro-deposition process was conducted under the potentials at -0.7 V(VS Ag/AgCl reference electrode). At this potential, both hydrogen evolution and metal Au deposition can take place. The evolved hydrogen form gas bubbles, and Au complex ions inside the electrolyte can be reduced by hydrogen atoms around the bubbles to form metal Au on the bubble boundary. The electro-deposition process time was controlled about 800 seconds. Hollow Au nanoparticles with a diameter of 120-150 nm formed on the wall of the channels of AAO. Then, to release the Au nanoparticles from AAO membrane channels, 2M NaOH was used to dissolve the membrane. Figure 4-2 shows the morphology of Au nanoparticles.

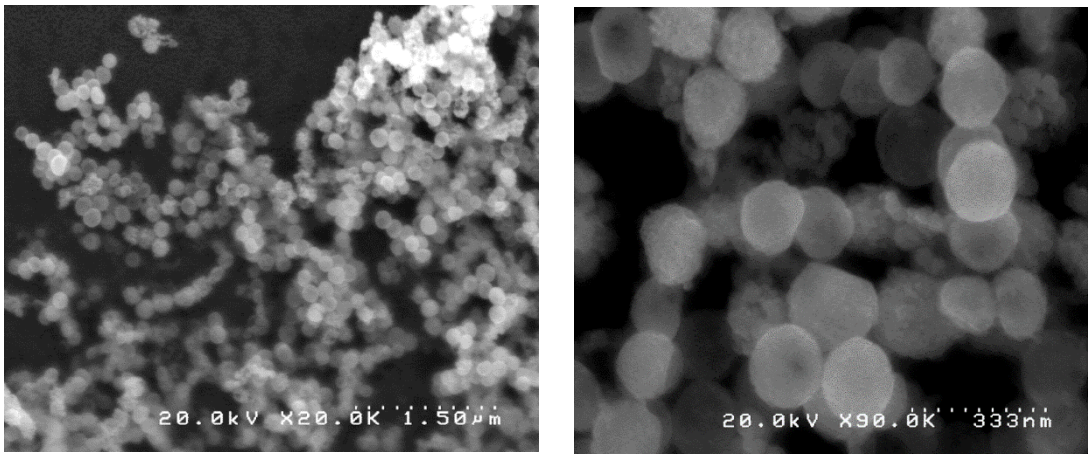

Figure 4- 2 SEM Images of Au Hollow Nanoparticles Synthesized at -0.7V And 800 Seconds.

4.1.2. Synthesis of Au/Cu Core-Shell Nanoparticles by Electroless Plating

The overall process of synthesis Au/Ag core-shell nanoparticles is shown in the following figure.

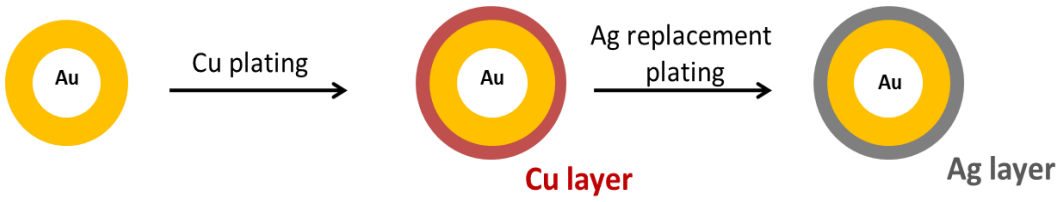

Figure 4- 3 Synthesis of Au/Ag Core-Shell Nanoparticles by Electroless Plating

First, the Cu shells will be plated on prepared Au nanoparticles surface via electroless deposition in Cu plating solution. Hollow gold nanoparticles inside template was immersed in a Cu plating electrolyte with different dipping time. The electrolyte include Cu metal ion and formaldehyde （reducing agent. Buffer solution (1M NaOH solution) and stabilizer were added to prevent copper precipitation during elctroless deposition. The composition of copper plating solution was showed in the table 4-1. This method was first discovered by A. Brenner and G.E. Riddell in 1950. Also, we can utilize different kinds of chemical solution to coat nickel, copper, silver, gold, or palladium shells on the metal surface.

Table 4- 1 Cu Plating Solution for Synthesizing Au/Cu Core Shell Nanoparticles

Metal Cu iron solution	Disodium salt dehydrate	Reducing agent	Buffer solution
0.4 M CuSO4	0.17 M EDTA	37% of original Formaldehyde	0.1M NaOH

Cu shell thickness can be controlled by the dipping time (10, 20, 30, 40, minutes). Hsu et.al demonstrated that the dipping time for 20 minutes was controllable and stable [38]. In this procedure, the vacuum filtration system was used for the purpose of force plating solution to go through the AAO membrane channels, where hollow Au nanoparticles exist.

Next, this Cu layer can be replaced by Ag through a galvanic replacement reaction in a AgCN based aqueous solution

A technical Redox (reduction-oxidation) reaction (galvanic replacement reaction) is the most commonly method of producing metallic nanoparticles. In general, redox reactions involve the transfer of electrons between species. It can be used to coat different kinds of metals on the surface according to the following galvanic replacement reaction:

$$A + BC \rightarrow AC + B$$

where A and B are metals and BC, AC are metal iron solutions, the requirement of this chemical reaction to happen is that A must be more active than B.

The standard reduction potential of different metals are showed in the Table 4-2.

Table 4- 2 The Standard Reduction Potential Reaction for Cu, Ag, Au Metals

Reaction Equation	E^0(V)
$Cu^{2+} + 2e^- \rightarrow Cu_{(s)}$	0.340
$Ag^+ + e^- \rightarrow Ag_{(s)}$	0.800
$Au^{3+} + 3e^- \rightarrow Au_{(s)}$	1.52

It can be seen that Cu shells can be replaced by Ag. This process is based on the following galvanic replacement reaction:

$$Cu_s + 2Ag_{aq}^+ \rightarrow 2Ag_s + Cu_{aq}^{2+}$$

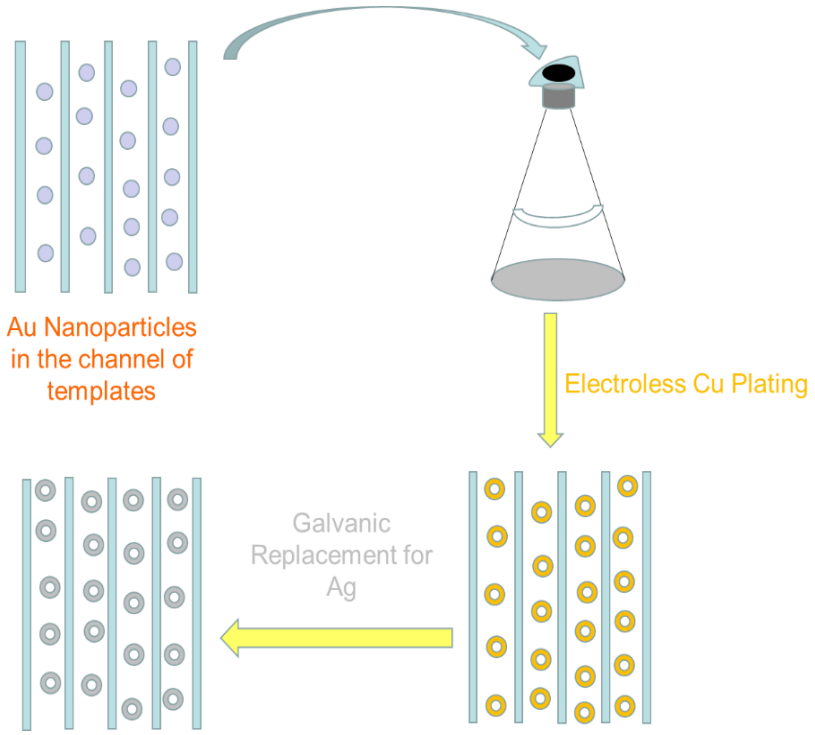

Figure 4- 4 The Schematic of Au/Ag Core-Shell Nanoparticles Were Synthesized by Galvanic Replacement Process.

Figure 4-4 shows the whole process to fabricate Au/Ag core-shell nanoparticles. After Au nanoparticles were formed inside the channels of AAO membrane, this membrane was carried to the top of the vacuum filtration system. Then the Cu plating solution were slowly sucked into AAO membrane, forcing solution go through the channels. The membrane with Au/Cu core-shell nanoparticles was rinsed by DI water using the same

vacuum filtration system. The finally step is that AgCN based solution was sucked through the channels to replace the Cu shells, and the Au/Ag core-shell nanoparticles can be obtained.

4.2 Characterization Of Au/Ag Core-Shell Nanoparticles

The morphology and composition of Au/Ag core-shell nanoparticles were examined by scanning electron microscopy (SEM), energy dispersive spectroscopy (EDS) and transmission electron spectroscopy(TEM).

4.2.1 Scanning Electron Microscopy

Figure 4-5 shows SEM images of Au/Ag core-shell nanoparticles. The average diameter of Au/Ag core-shell nanoparticle is about 150 nm. The nanoparticles have a rough surface.

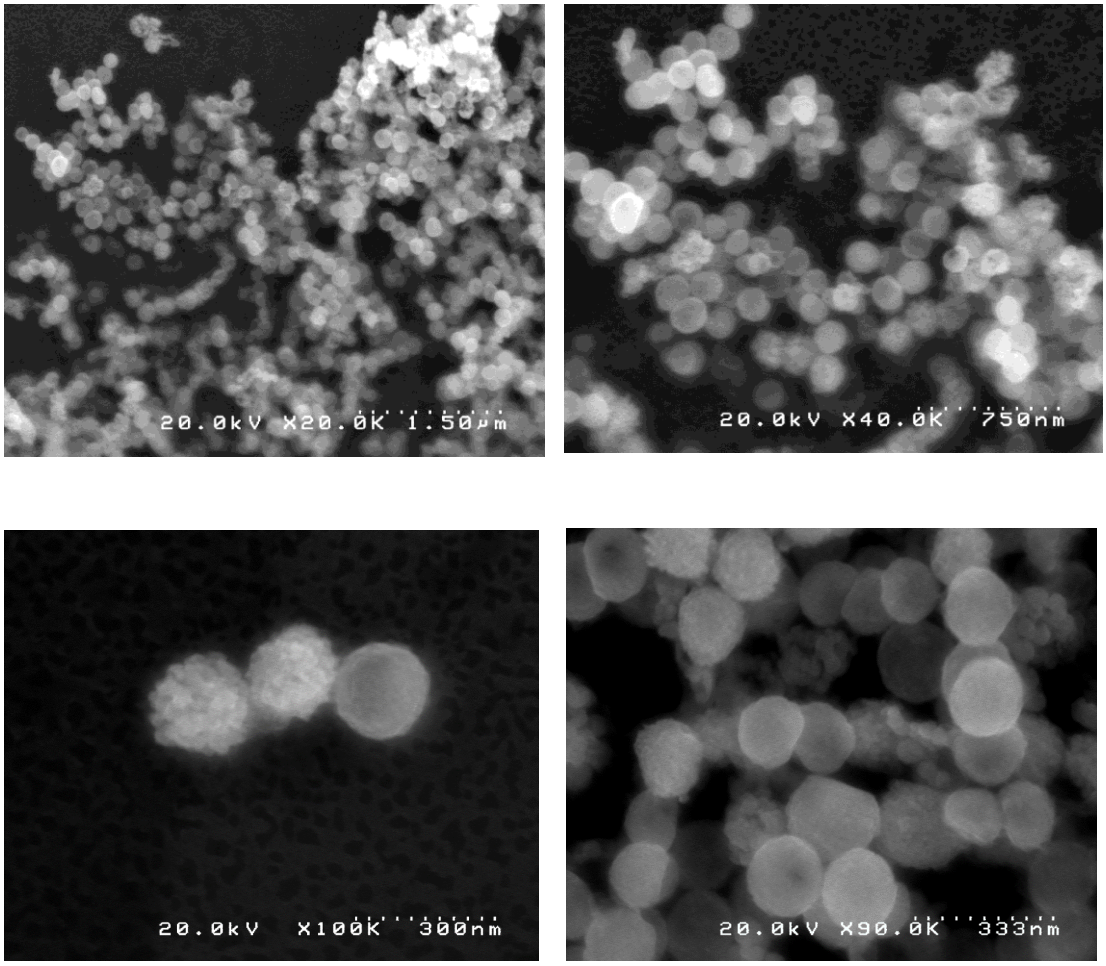

Figure 4- 5 SEM Images of Synthesized Au/Ag Core-Shell Nanoparticles.

4.2.2 Energy Dispersive Spectroscopy

To confirm Ag shells on the surface of core Au nanoparticles, the energy dispersive spectroscopy was used to examine Au/Ag core-shell

nanoparticles. As shown in Figure 4-6 below, we can easily see Au and Ag signal from the prepared nanoparticles.

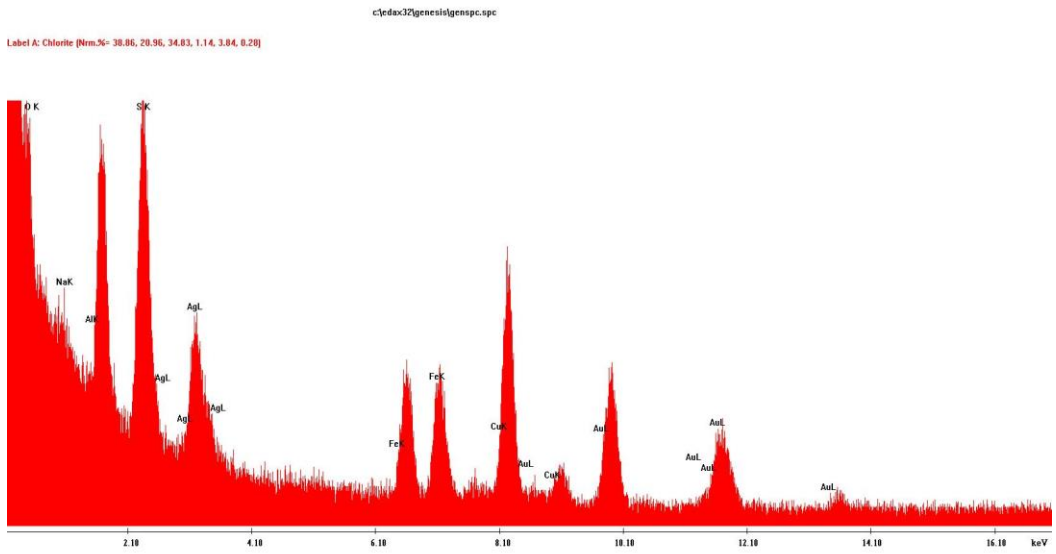

Figure 4- 6 EDS Spectrum of Au/Ag Core-Shell Nanoparticles

4.2.3 Transmission Electron Microscopy

Au/Ag core-shell nanoparticles were also examined by high resolution TEM. Figure 4-7 shows TEM images of Au/Ag core-shell nanoparticles which were synthesized in 70% AgCN solution for 20 minutes. The figure clearly shows 30 nm thickness of Ag shell on the Au core nanoparticles. The average diameter of Au/Ag core-shell nanoparticles is about 150 nm. Also, it

can be seen that the surface of silver shells is rough, which can further enhance Raman signal in SERS test.

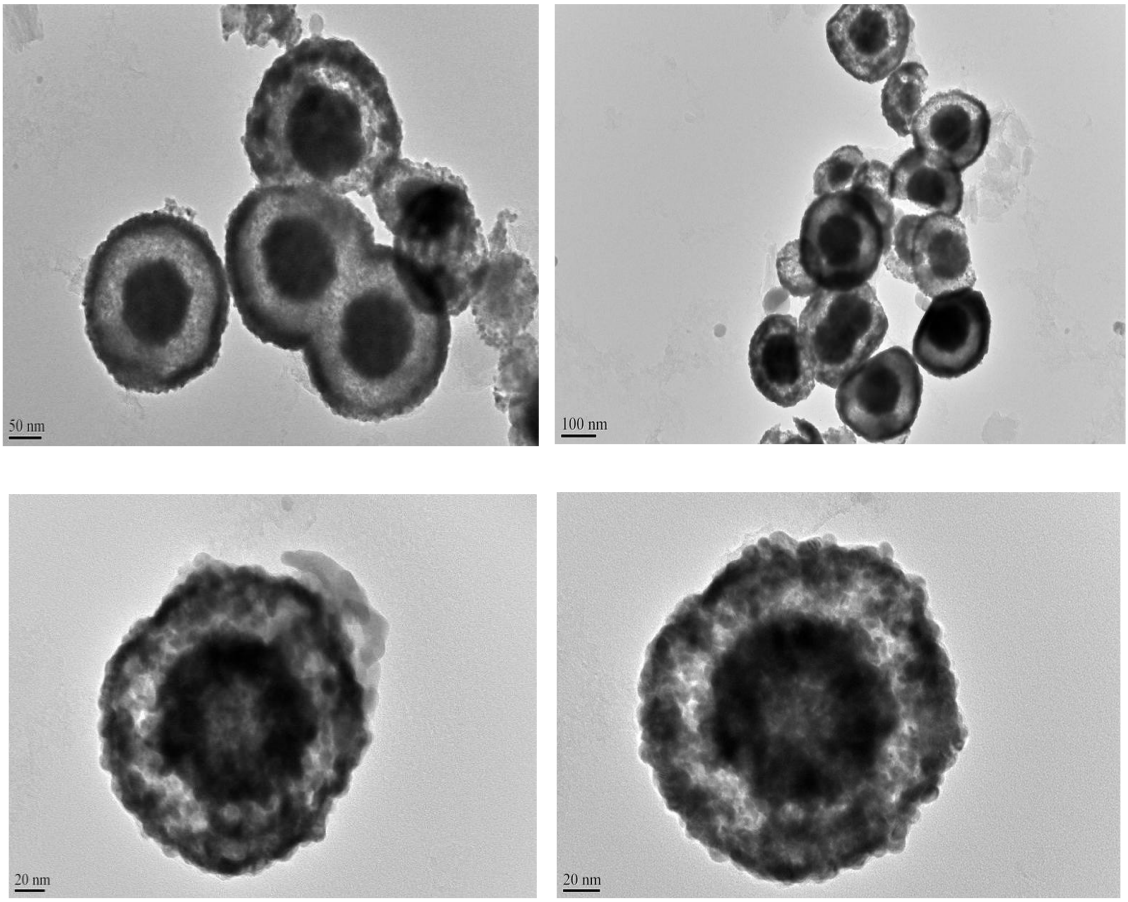

Figure 4- 7 TEM Images of Synthesized Au/Ag Core-Shell Nanoparticles

4.2.4 Plasmonic Properties of Au/Ag Core-Shell Nanoparticles

As described above, Au/Ag core-shell nanoparticles can be successfully obtained by this simple electroless deposition method. The Au/Ag core-shell nanoparticles can be released from the membrane by immersing the membranein 2 M NaOH solution for twenty minutes. The Au/Ag core-shell nanoparticles were collected from the bottom of the solution after these nanoparticles settled down. After that, these nanoparticles were rinsed three times by deionized water and centrifugation at 8500 rpm speed for 15 minutes. Then Au/Ag core-shell nanoparticles suspension were mixed with 10^{-4} M DTTC dye solution for three hours under the air condition at the room temperature. Figure 4-8 shows the process of the preparation for Raman measurement.

Figure 4- 8 Au/Ag Core-Shell Nanoparticles Are Prepared for Raman Measurements

The prepared aqueous solution sample was dropped on the surface of glass slide. The Raman spectroscopy measurement was conducted using a DXR thermo Raman microscopy with a 532 nm laser. The Raman signal were collected with 8s of exposure time. And the laser power is 50 mW. The Raman spectrum of Au/Ag core-shell nanoparticles with 1×10^{-4} M DTTC displayed the major vibrational modes of DTTC in the Figure 4-9.

We can see there is a significant enhancement when compare with Raman results of using hollow Au nanoparticles and DTTC alone. This results indicate the steady absorption of Raman dyes on the surface of

Au/Ag core-shell nanoparticles and have a good performance in surface-enhanced Raman spectroscopy.

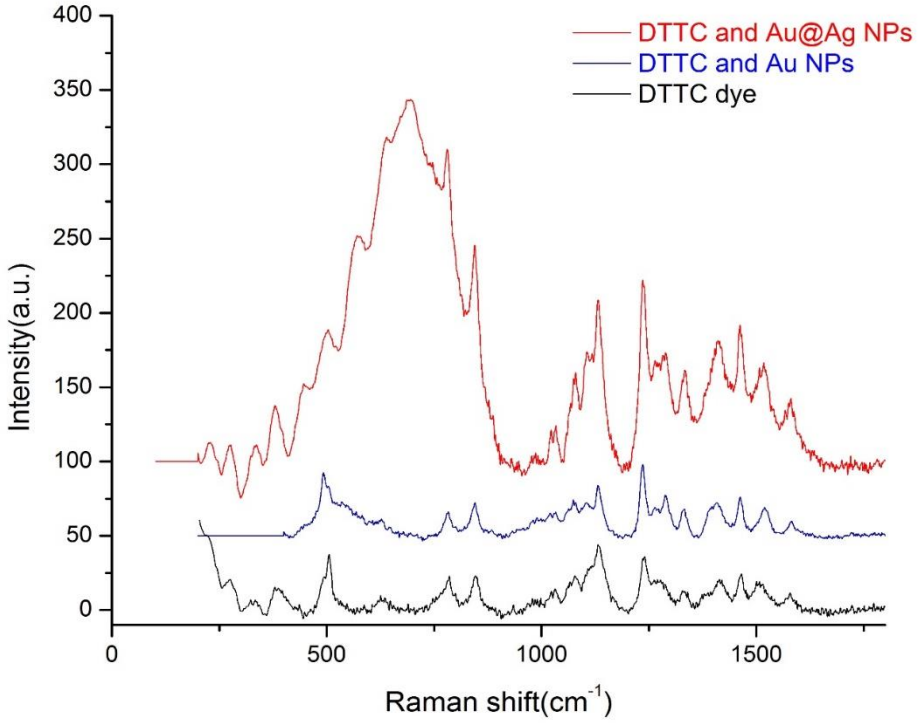

Figure 4- 9 SERS Spectra of DTTC Molecules

Chapter 5

Conclusion

In this thesis, we demonstrated two simple methods to make different plasmonic nanostructures. The first one is the fabrication of Ag dendrites on the top of AAO membrane by galvanic reaction. The other one is the fabrication of Au/Ag core-shell nanoparticles by electroless deposition process. These plasmonic nanostructures can be used for SERS substrates. Ag dendrites and Au/Ag core-shell nanoparticles can serve as substrates to enhance Raman signal for molecules with a low concentration.

In recent years, Ag dendrites have been formed on metal Cu surface by replacement reaction with $AgNO_3$. The process developed here successfully separate Ag dendrites from the reactant Cu metal. The mechanism of Ag dendrites forming on the top of AAO membrane were discussed in this thesis. This approach can be considered as a galvanic cell. Produced Ag dendrite is single crystal nanostructure, which were confirmed by XRD, electron diffraction pattern and TEM dark field images. Furthermore, Ag dendrites have shown a good performance to serve as a substrate in surface-enhanced Raman spectroscopy.

We also developed a simple method to produce Au/Ag core-shell nanoparticles. In this process, the Au/Cu core-shell nanoparticles were first synthesized. Then, the Ag shells were formed by replacing Cu shells with

silver in AgCN solution. DTTC dye adsorbed on such novel nanostructure show significantly enhanced Raman signal when compared with the signal from DTTC alone.

References

[1]. Barnes WL, Dereux A, Ebbesen TW. Surface plasmon subwavelength optics. *Nature* 2003; **424**(6950): 824-30.

[2]. Ozbay E. Plasmonics: merging photonics and electronics at nanoscale dimensions. *science* 2006; **311**(5758): 189-93.

[3]. Boltasseva A, Atwater HA. Low-loss plasmonic metamaterials. *Science* 2011.

[4]. Geneviève M, Vieu C, Carles R, et al. Biofunctionalization of gold nanoparticles and their spectral properties. *Microelectronic engineering* 2007; **84**(5): 1710-3.

[5]. Bozhevolnyi SI, Volkov VS, Devaux E, Laluet J-Y, Ebbesen TW. Channel plasmon subwavelength waveguide components including interferometers and ring resonators. *Nature* 2006; **440**(7083): 508-11.

[6]. Hu M, Chen J, Li Z-Y, et al. Gold nanostructures: engineering their plasmonic properties for biomedical applications. *Chemical Society Reviews* 2006; **35**(11): 1084-94.

[7]. Chang S-H, Nyagilo J, Wu J, Hao Y, Davé D. Optical Fiber-Based Surface-Enhanced Raman Scattering Sensor Using Au Nanovoid Arrays. *Plasmonics* 2012; **7**(3): 501-8.

[8]. Albrecht MG, Creighton JA. Anomalously intense Raman spectra of pyridine at a silver electrode. *Journal of the American Chemical Society* 1977; **99**(15): 5215-7.

[9]. Yang J, Palla M, Bosco FG, et al. Surface-Enhanced Raman Spectroscopy Based Quantitative Bioassay on Aptamer-Functionalized Nanopillars Using Large-Area Raman Mapping. *ACS nano* 2013; **7**(6): 5350-9.

[10]. Deng Y-L, Juang Y-J. Black silicon SERS substrate: Effect of surface morphology on SERS detection and application of single algal cell analysis. *Biosensors and Bioelectronics* 2014; **53**(0): 37-42.

[11]. Xue C, Millstone JE, Li S, Mirkin CA. Plasmon‐Driven Synthesis of Triangular Core‐Shell Nanoprisms from Gold Seeds. *Angewandte Chemie* 2007; **119**(44): 8588-91.

[12]. Nath N, Chilkoti A. A colorimetric gold nanoparticle sensor to interrogate biomolecular interactions in real time on a surface. *Analytical Chemistry* 2002; **74**(3): 504-9.

[13]. Tan YN, Su X, Zhu Y, Lee JY. Sensing of transcription factor through controlled-assembly of metal nanoparticles modified with segmented DNA elements. *ACS nano* 2010; **4**(9): 5101-10.

[14]. Larsson EM, Alegret J, Käll M, Sutherland DS. Sensing characteristics of NIR localized surface plasmon resonances in gold nanorings for application as ultrasensitive biosensors. *Nano letters* 2007; **7**(5): 1256-63.

[15]. Liu N, Mesch M, Weiss T, Hentschel M, Giessen H. Infrared perfect absorber and its application as plasmonic sensor. *Nano letters* 2010; **10**(7): 2342-8.

[16]. Stewart ME, Anderton CR, Thompson LB, et al. Nanostructured plasmonic sensors. *Chemical reviews* 2008; **108**(2): 494-521.

[17]. Wokaun A, Gordon J, Liao P. Radiation damping in surface-enhanced Raman scattering. *Physical Review Letters* 1982; **48**(14): 957.

[18]. Bell SE, Sirimuthu NM. Surface-enhanced Raman spectroscopy (SERS) for sub-micromolar detection of DNA/RNA mononucleotides. *Journal of the American Chemical Society* 2006; **128**(49): 15580-1.
[19]. Doering WE, Piotti ME, Natan MJ, Freeman RG. SERS as a foundation for nanoscale, optically detected biological labels. *Advanced Materials* 2007; **19**(20): 3100-8.
[20]. Schatz GC, Young MA, Van Duyne RP. Electromagnetic mechanism of SERS. Surface-enhanced Raman scattering: Springer; 2006: 19-45.
[21]. Fievet F, Lagier J, Figlarz M. Preparing monodisperse metal powders in micrometer and submicrometer sizes by the polyol process. *Mrs Bulletin* 1989; **14**(12): 29-34.
[22]. Marinakos SM, Chen S, Chilkoti A. Plasmonic detection of a model analyte in serum by a gold nanorod sensor. *Analytical chemistry* 2007; **79**(14): 5278-83.
[23]. Sers C, Kirsch K, Rothbächer U, Riethmüller G, Johnson JP. Genomic organization of the melanoma-associated glycoprotein MUC18: implications for the evolution of the immunoglobulin domains. *Proceedings of the National Academy of Sciences* 1993; **90**(18): 8514-8.
[24]. Tsuji M, Matsuo R, Jiang P, et al. Shape-dependent evolution of Au@ Ag core− shell nanocrystals by PVP-assisted N, N-dimethylformamide reduction. *Crystal Growth and Design* 2008; **8**(7): 2528-36.
[25]. Wang D, Hao Y, Zhu X, et al. FPGA implementation of hardware processing modules as coprocessors in brain-machine interfaces. Engineering in Medicine and Biology Society, EMBC, 2011 Annual International Conference of the IEEE; 2011: IEEE; 2011. p. 4613-6.
[26]. Sers C, Husmann K, Nazarenko I, et al. The class II tumour suppressor gene H-REV107-1 is a target of interferon-regulatory factor-1 and is involved in IFNgamma-induced cell death in human ovarian carcinoma cells. *Oncogene* 2002; **21**(18): 2829-39.
[27]. Sers C, Emmenegger U, Husmann K, Bucher K, Andres A-C, Schäfer R. Growth-inhibitory activity and downregulation of the class II tumor-suppressor gene H-rev107 in tumor cell lines and experimental tumors. *The Journal of cell biology* 1997; **136**(4): 935-44.
[28]. Otto A. Surface-enhanced Raman scattering:“classical” and “chemical” origins. Light scattering in solids IV: Springer; 1984: 289-418.
[29]. Schatz GC, Van Duyne RP. Electromagnetic Mechanism of Surface‐Enhanced Spectroscopy. *Handbook of vibrational spectroscopy* 2002.
[30]. Etchegoin P, Cohen L, Hartigan H, Brown R, Milton M, Gallop J. Electromagnetic contribution to surface enhanced Raman scattering revisited. *The Journal of chemical physics* 2003; **119**(10): 5281-9.
[31]. Le Ru E, Etchegoin P. Principles of Surface-Enhanced Raman Spectroscopy: and related plasmonic effects: Elsevier; 2008.
[32]. Michaels AM, Nirmal M, Brus L. Surface enhanced Raman spectroscopy of individual rhodamine 6G molecules on large Ag nanocrystals. *Journal of the American Chemical Society* 1999; **121**(43): 9932-9.
[33]. Norrod KL, Sudnik LM, Rousell D, Rowlen KL. Quantitative comparison of five SERS substrates: sensitivity and limit of detection. *Applied spectroscopy* 1997; **51**(7): 994-1001.

[34]. Moody R, Vo-Dinh T, Fletcher W. Investigation of experimental parameters for surface-enhanced Raman scattering (SERS) using silver-coated microsphere substrates. *Applied spectroscopy* 1987; **41**(6): 966-70.
[35]. Johnson J, Lehmann J, Stade B, Rothbächer U, Sers C, Riethmüller G. Functional aspects of three molecules associated with metastasis development in human malignant melanoma. *Invasion & metastasis* 1988; **9**(6): 338-50.
[36]. Liu T-Y, Tsai K-T, Wang H-H, et al. Functionalized arrays of Raman-enhancing nanoparticles for capture and culture-free analysis of bacteria in human blood. *Nature communications* 2011; **2**: 538.
[37]. Du Y, Shi L, He T, Sun X, Mo Y. SERS enhancement dependence on the diameter and aspect ratio of silver-nanowire array fabricated by anodic aluminium oxide template. *Applied Surface Science* 2008; **255**(5): 1901-5.
[38]. Hsu C, Huang C, Hao Y, Liu F. Au/Pd core–shell nanoparticles for enhanced electrocatalytic activity and durability. *Electrochemistry Communications* 2012; **23**: 133-6.

Biographical Information

Ruiqian Jiang was born in Hunan province, China. He received his B.S. in Mechanical Engineering from Hunan University of Arts and Science in 2012. After that, he began the study for his master degree in Materials Science and Engineering in University of Texas at Arlington in Dr.Yaowu Hao's group. During his master education, he was a treasurer in American Society Materials student organization and he served as a volunteer for summer camps in 2013 and 2014. He did a poster presentation in the Texas Society Microscopy meeting in 2014. His research field was related to the fabrication of plasmonic structures and their application in surface-enhanced Raman spectroscopy. He is familiar with electro-deposition and electroless plating process for nanostructures. As a master graduate student, he has ability to analyze the different structures through different techniques such as scanning electron microscopy (SEM), X-ray diffraction (XRD), transmission electron microscopy (TEM) and energy dispersive spectrometer (EDS), Raman spectroscopy and UV-vis spectroscopy.